Supporting Information

Distinctive Viewpoint on the Rapid Dissolution Mechanism of α-Chitin in Aqueous Potassium Hydroxide–Urea Solution at Low Temperatures

Junchao Huang,[§,‡] Yi Zhong,[§,‡] Lina Zhang,[‡,†] and Jie Cai*[,‡,†]

[‡] College of Chemistry and Molecular Sciences, Wuhan University, Wuhan 430072, China

[†] Hubei Engineering Center of Natural Polymer-based Medical Materials, Wuhan University, Wuhan 430072, China

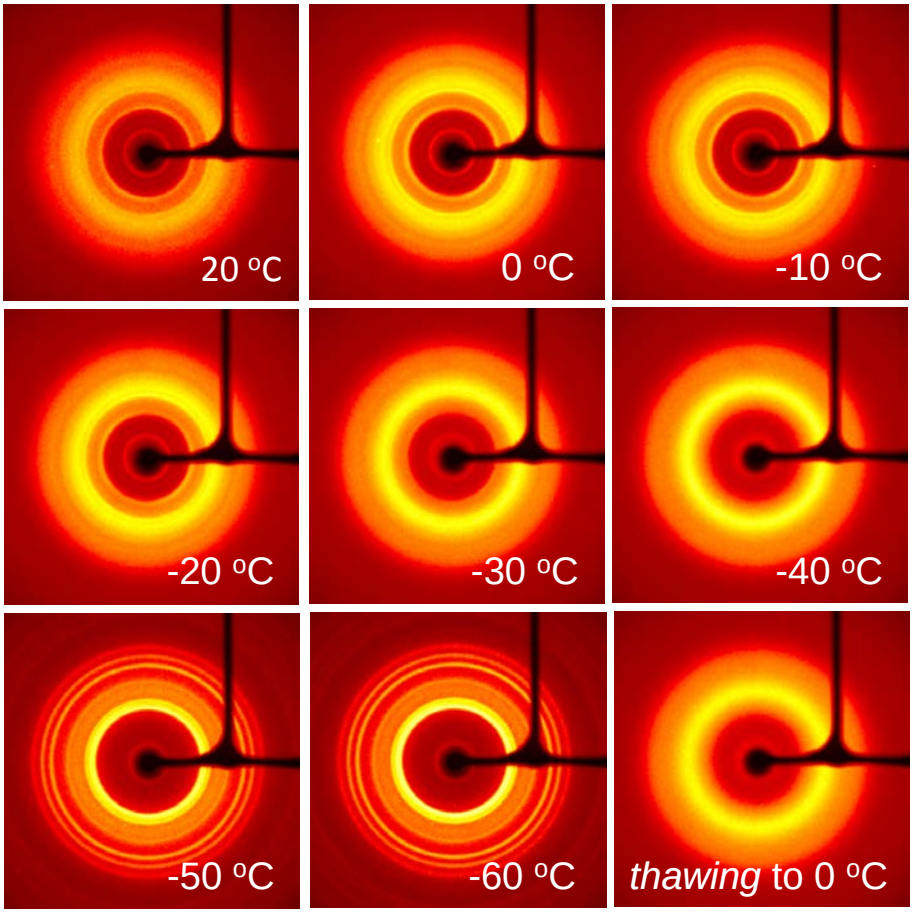

Figure S1. 2D WAXD patterns of α-chitin dissolved in 20 wt.% (3.6 M) aqueous KOH solution at different temperatures.

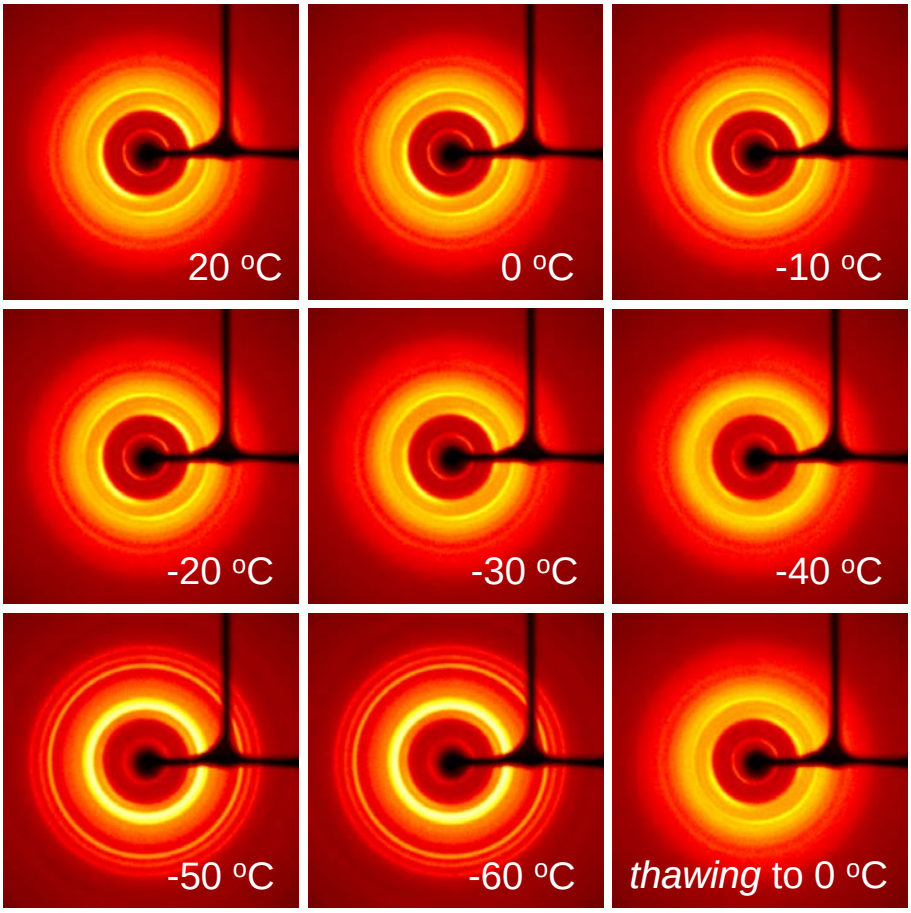

Figure S2. 2D WAXD patterns of α-chitin powder in 14.4 wt.% (3.6 M) aqueous NaOH solution at different temperatures.

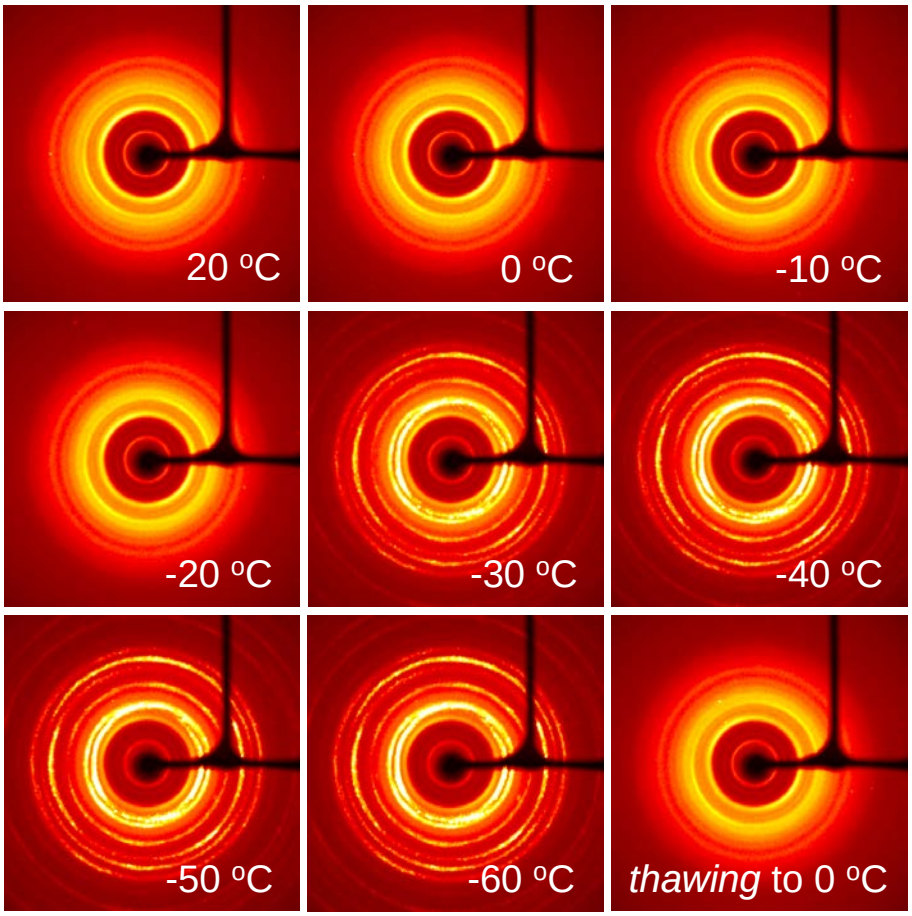

Figure S3. 2D WAXD patterns of α-chitin powder in 8.6 wt.% (3.6 M) aqueous LiOH solution at different temperatures.

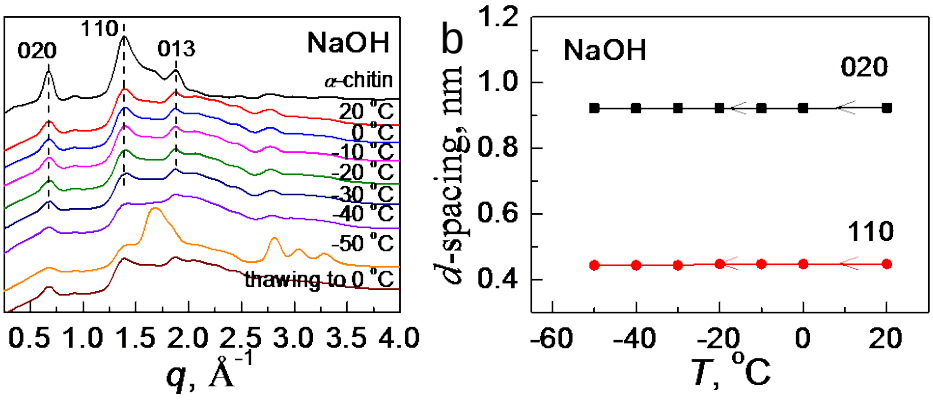

Figure S4. (a) Equatorial XRD profiles of α-chitin powder and α-chitin in the aqueous NaOH solution obtained during cooling from 20 to -50 °C and then thawing to 0 °C. The term q denotes the scattering vector ($2\pi/d$). (b) Changes in the d-spacing between the (020) and (110) planes during cooling the aqueous NaOH solutions from 20 to -50 °C calculated from the XRD profiles.

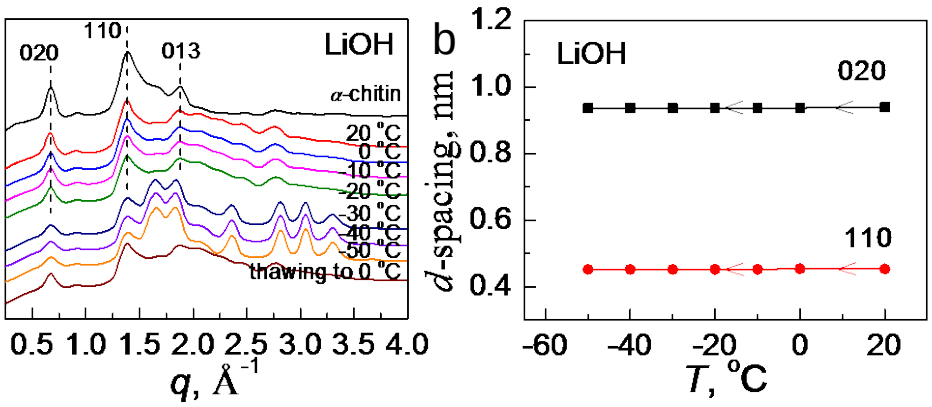

Figure S5. (a) Equatorial XRD profiles of α-chitin powder and α-chitin in the aqueous LiOH solution obtained during cooling from 20 to -50 °C and then thawing to 0 °C. The term q denotes the scattering vector ($2\pi/d$). (b) Changes in the d-spacing between the (020) and (110) planes during cooling the aqueous LiOH solution from 20 to -50 °C calculated from the XRD profiles.

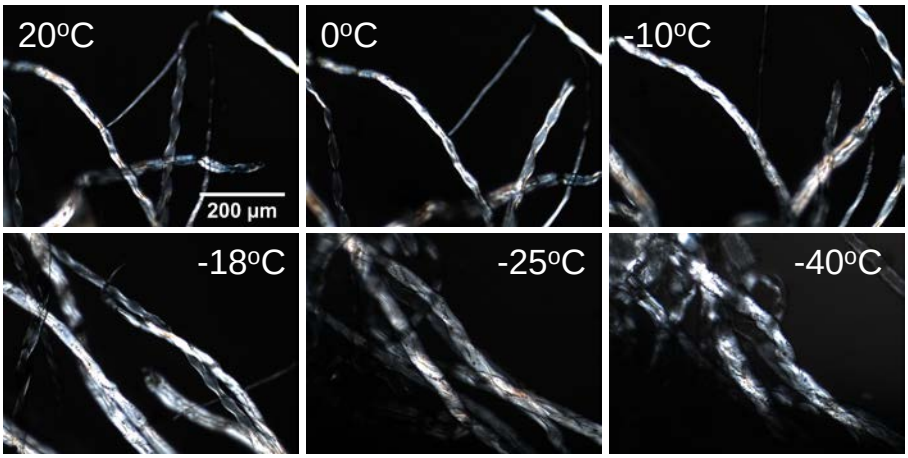

Figure S6. Polarizing microscopy images of cellulose I in the aqueous KOH aqueous solution at different temperatures.

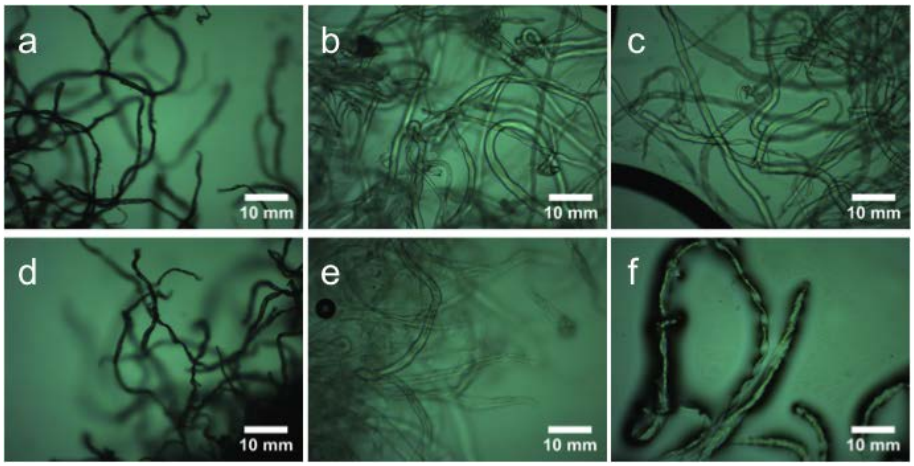

Figure S7. (a-c) Optical microscopy images of cellulose I (a), cellulose I in the aqueous KOH solution at -30 °C for 30 min (b) and 90 min (c). **(d-f)** Optical microscope images of cellulose II (d), and cellulose II in the aqueous KOH solution at -30 °C for 30 min (e) and 90 min (f).

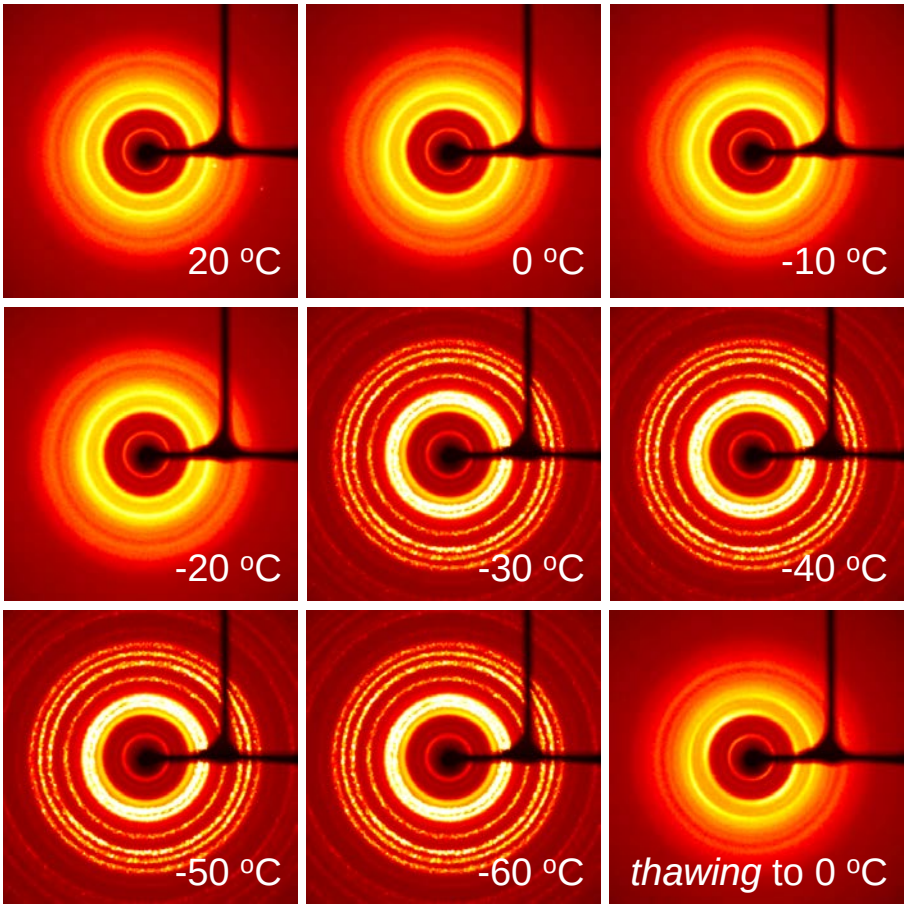

Figure S8. 2D WAXD patterns of α-chitin powder in 4 wt.% aqueous urea solution at different temperatures.

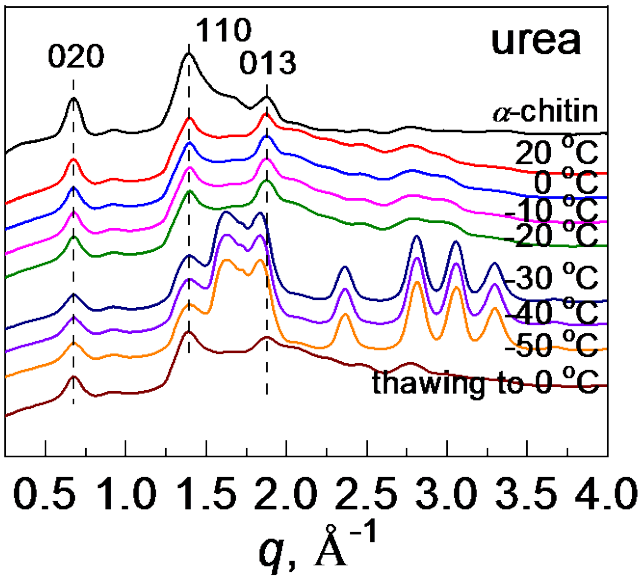

Figure S9. Azimuthal averaging XRD profiles of α-chitin powder and α-chitin in the aqueous urea solution during cooling from 20 to -50 °C and then thawing to 0 °C. The term q denotes the scattering vector ($2\pi/d$).

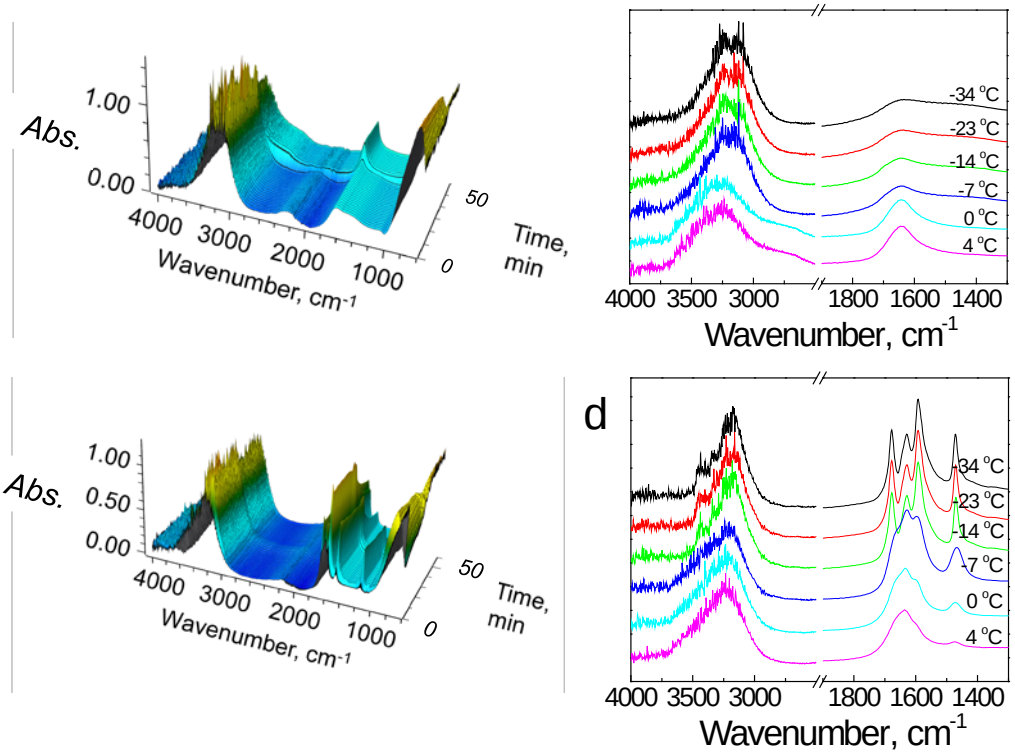

Figure S10. 3D FT-IR spectra of the KOH (a) and urea (b) aqueous solutions obtained by conducting time-course measurements. FT-IR spectra of the KOH (c) and urea (d) aqueous solutions extracted from the 3D FT-IR spectra recorded at different temperatures.

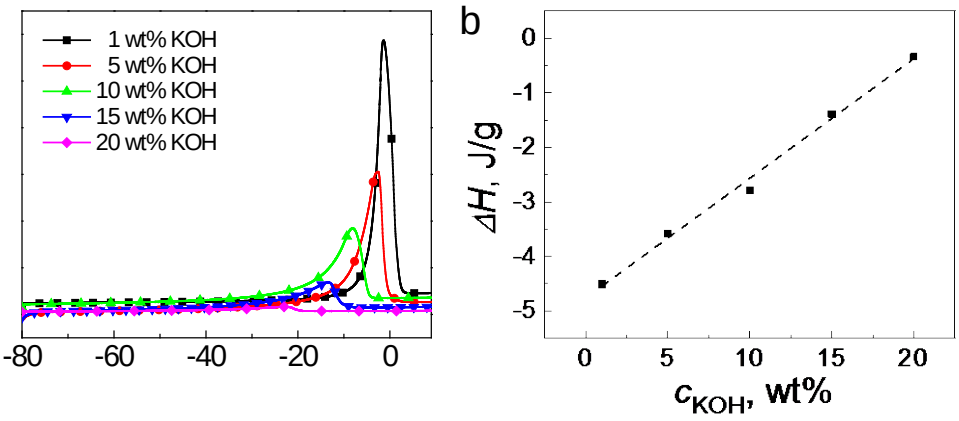

Figure S11. (a) DSC thermograms of aqueous KOH solutions with different concentrations. (b) Dependence of the enthalpy for free water on KOH concentration in aqueous KOH solution.

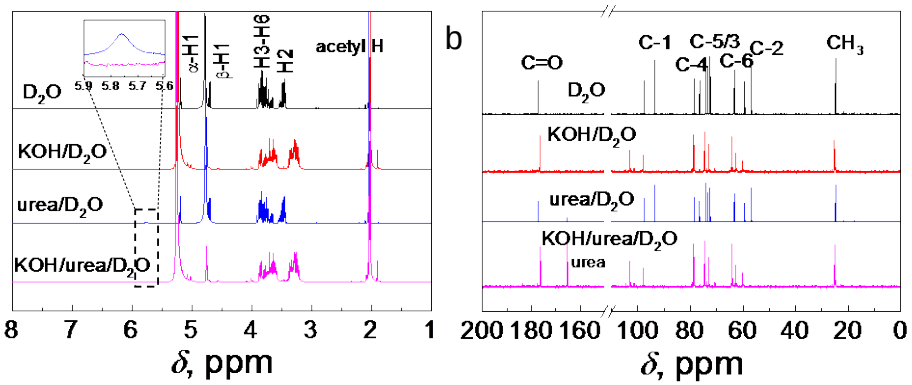

Figure S12. (a) ^{1}H, and (b) ^{13}C NMR spectra of GlcNAc in D_2O, KOH/D_2O, urea/D_2O and KOH/urea/D_2O solutions. The insert is the ^{1}H NMR spectra of amide proton of urea in urea/D_2O and KOH/urea/D_2O solutions.

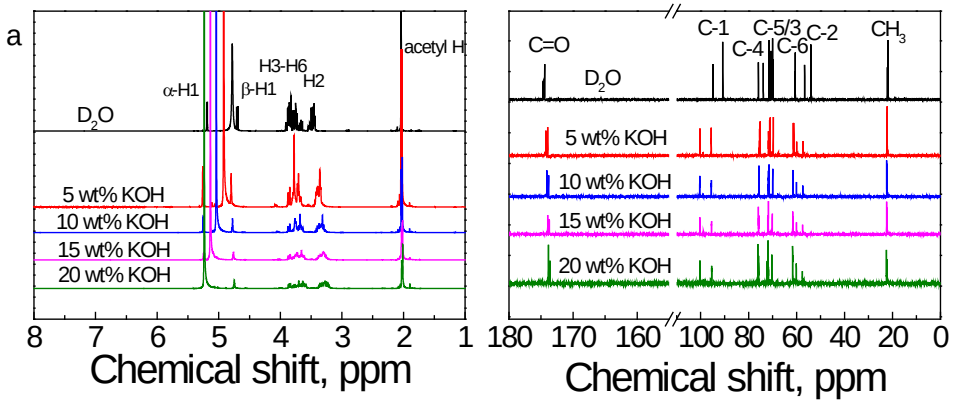

Figure S13. (a) ^{1}H, and (b) ^{13}C NMR spectra of GlcNAc dissolved in D_2O and KOH/D_2O solutions with different KOH concentrations.

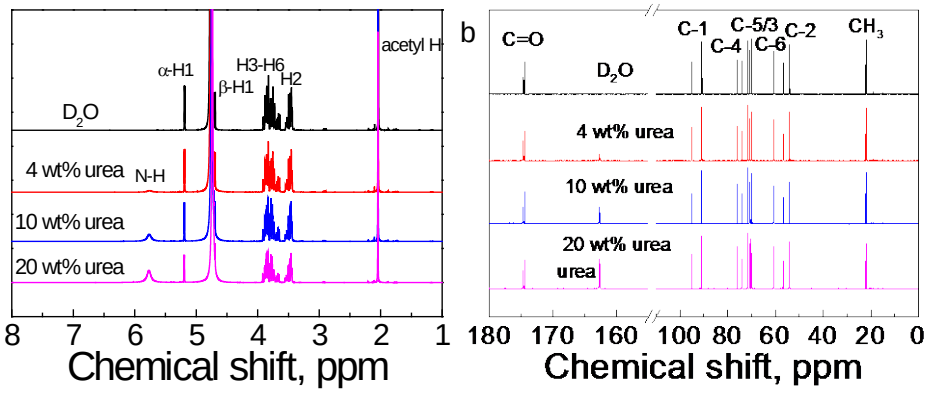

Figure S14. (a) ^{1}H, and (b) ^{13}C NMR spectra of GlcNAc dissolved in D_2O and urea/D_2O solutions with different urea concentrations.

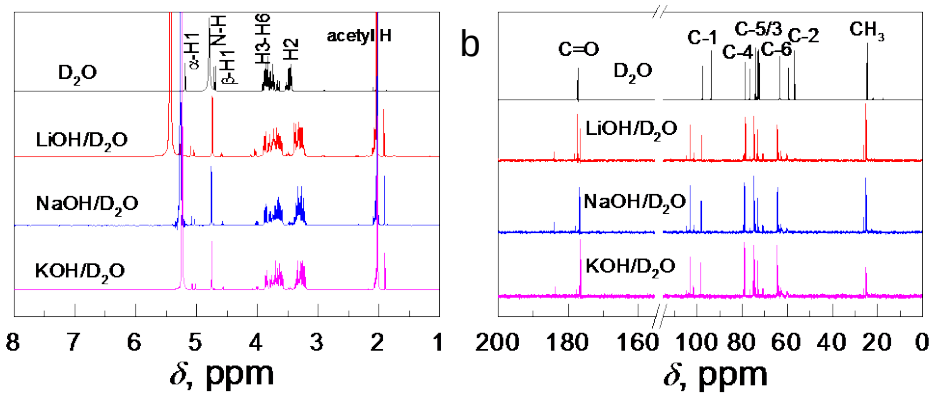

Figure S15. (a) ^{1}H, and (b) ^{13}CNMR spectra of GlcNAc in D_2O, $LiOH/D_2O$, $NaOH/D_2O$ and KOH/D_2O solutions.

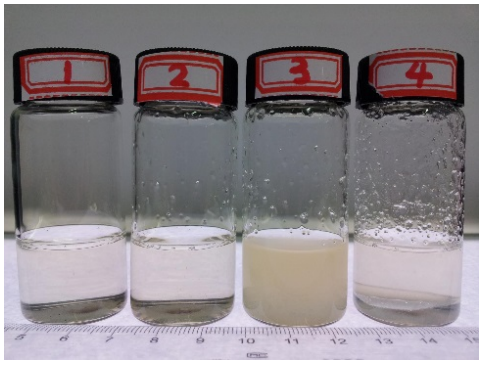

Figure S16. From left to right: Photographs of the α-chitin dissolved in aqueous KOH solution (sample 1), and with addition of 12-Crown-4 (sample 2), 15-Crown-5 (sample 3) and 18-Crown-6 (sample 4), respectively. The molar ratio of the crown ethers to KOH is 1:10. Specifically, the 15-Crown-5 is slightly soluble in water.